Instrument Response Functions of the Antarctic Demonstrator for the Advanced Particle-astrophysics Telescope

Wenlei Chen[1], James Buckley[2], Marion Sudvarg[2], and Davide Serini[3] for the APT Collaboration†

[1]Department of Physics, Oklahoma State University, Stillwater, OK 74078, USA; [2]Department of Physics, Washington University in St. Louis, St. Louis, MO 63130, USA ; [3]Istituto Nazionale di Fisica Nucleare, Sezione di Bari, 70125 Bari, Italy

The Advanced Particle-astrophysics Telescope (APT) and the Antarctic Demonstrator for the APT (ADAPT)

• Advanced Particle-astrophysics Telescope

- The Advanced Particle-astrophysics Telescope (APT) is a proposed gamma-ray and cosmic-ray observatory planned for orbit around the sun-Earth L2 point. Using a multilayer tracker and an imaging calorimeter, APT will detect gamma rays from hundreds of keV to a few TeV. Its design features 3-meter scintillating fibers with silicon photomultiplier readouts, maximizing the effective area and field of view. The detector combines scintillating fiber trackers with a calorimeter made of thin sodium-doped CsI layers and crossed wavelength-shifting (WLS) fibers for precise energy measurements.

• Antarctic Demonstrator for the APT

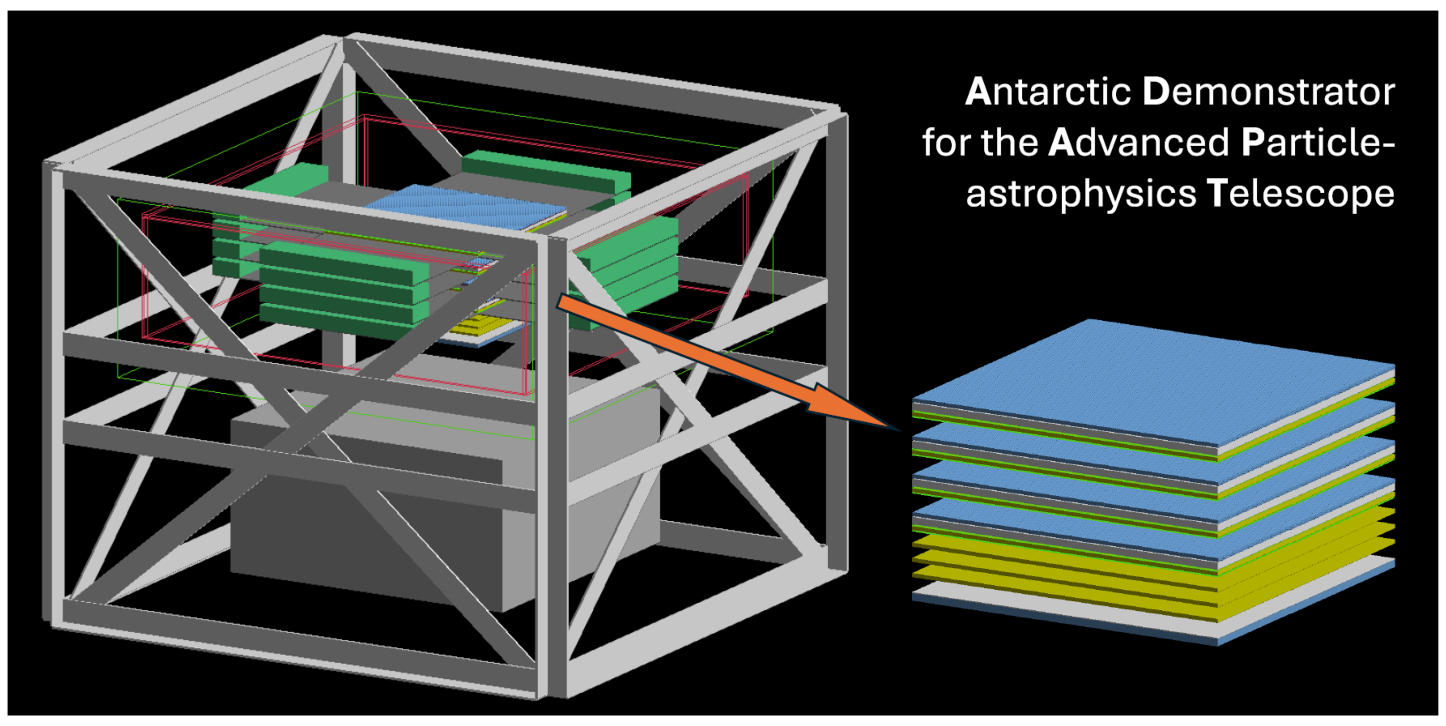

- To validate the capabilities of the APT instrument and to evaluate gamma-ray and cosmic-ray reconstruction algorithms, we designed the Antarctic Demonstrator for APT (ADAPT), which is a high-altitude balloon experiment that utilizes approximately 1% of the sensitive material incorporated in the complete APT detector. The mission will offer real-time alerts and localization for gamma-ray bursts (GRBs) and other gamma-ray transients detected during the planned Antarctic flight.
- The sensitive detector of ADAPT consists of 4 fully instrumented tracker/imaging-CsI-calorimeter (ICC) layers and 4 additional CsI-calorimeter layers on bottom to increase the radiation length of the instrument. Each CsI-calorimeter layer includes 3×3 tiles of 15cm × 15cm × 5mm CsI:Na crystals. The design will achieve a ∼ 0.5-meter square aperture for gamma-ray and cosmic-ray observations. A 1 mm tungsten sheet with 1 cm thick scintillator is placed beneath the calorimeter layers for additional albedo radiation veto.

Simulation and Reconstruction of Gamma-Ray Events

- Gamma-ray and cosmic-ray events for the APT and ADAPT detectors are simulated using Geant4.
- The APT instrument operates as both a pair telescope for 30 MeV to 1 TeV gamma rays and a Compton telescope with sensitivity down to ∼ 0.3 MeV. Pair production dominates above 30 MeV, while below 10 MeV, gamma rays primarily undergo multiple Compton scatterings before depositing energy or escaping. Reconstruction methods for Compton and pair events differ, resulting in an energy gap at ∼ 10-30 MeV where neither mode is effective.
- Using realistic and optimized models of optical signals, measurements of energy deposition are calibrated by correcting for fiber attenuation loss and dark counts. During a gamma ray event, the optical signals collected are significantly affected by the noise of dark counts and optical contamination. To implement event-reconstruction algorithms, signal islands are identified to enable accurate measurement of the particle shower in the detector.

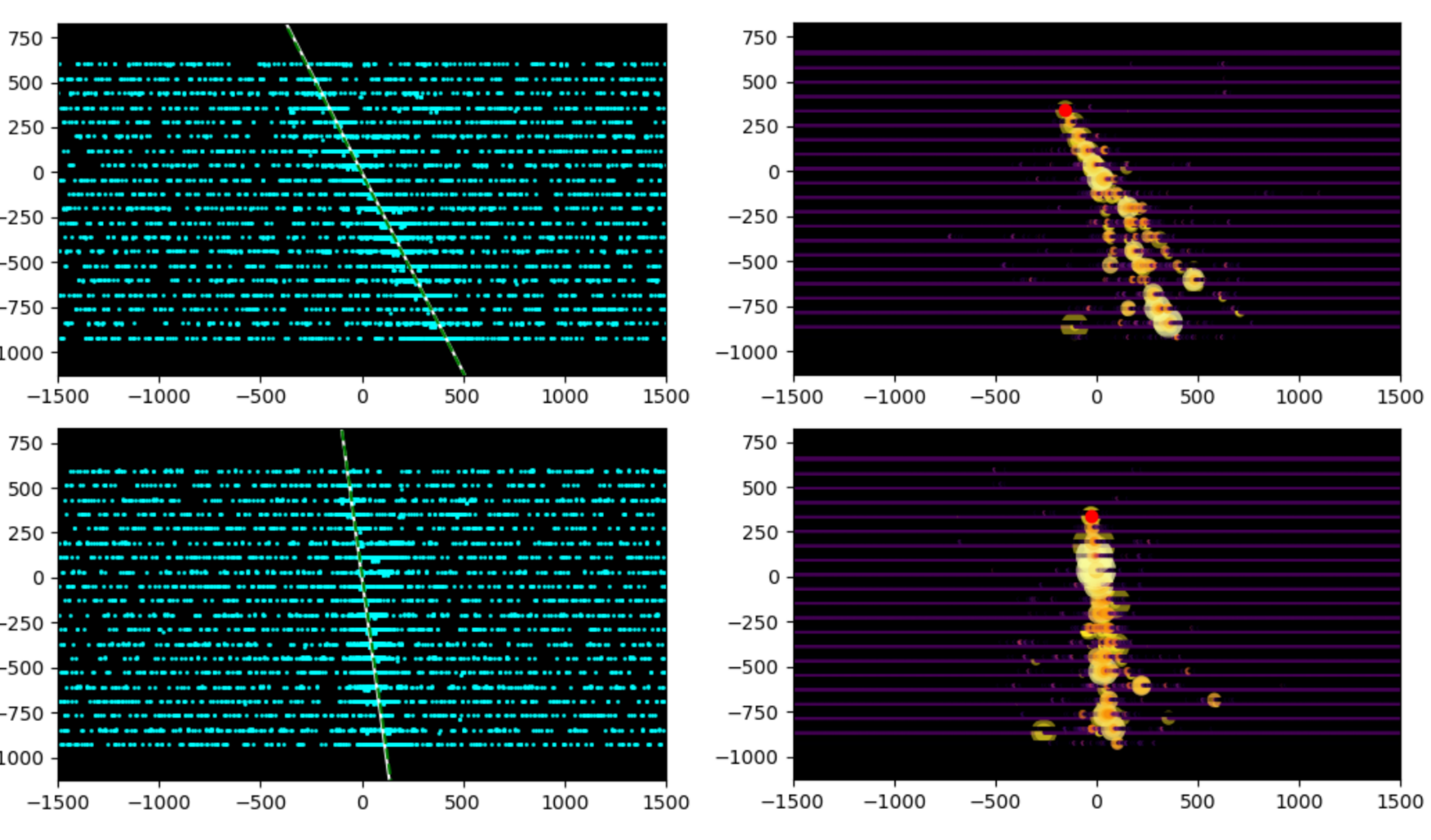

An example of a 1 GeV gamma-ray event recorded by the APT detector: The two panels on the left display the XZ-plane and YZ-plane channels that detect optical signals during the event. The two panels on the right show the corresponding signal islands identified for this event, where the size and color of each island in the figure indicate the width and intensity, respectively. The red dots marked in the right panels denote the primary hits detected in the XZ and YZ planes. The coordinates are given in mm.

Instrument Response Functions (IRFs)

• Overview

- Instrument performance is assessed by statistically calculating the differences between parameters obtained from simulated gamma rays and those obtained from reconstructed events. The IRFs for APT and ADAPT in detecting gamma rays are characterized by three key factors: efficiency of the gamma-ray detection represented by the effective area, angular resolution measured by the PSF, and energy resolution represented by the energy dispersion.

• Effective Area and Geometric Factor

- The effective area is a crucial aspect of the IRF that quantifies the capability of a gamma-ray telescope to detect resolvable gamma rays. The key parameters affecting detection efficiency are the angle of inclination relative to the detector's Z-axis (θ) and the energy (E) of the incident gamma ray.
- Detection efficiency is assessed across the full range of these parameters to provide comprehensive coverage for both the APT and the ADAPT instruments. For each inclination angle bin, 10^6 gamma rays are generated over the energy range of 0.3 MeV to 1 TeV. The dependence of the azimuthal angle φ in the effective area is negligible relative to the statistical fluctuations.

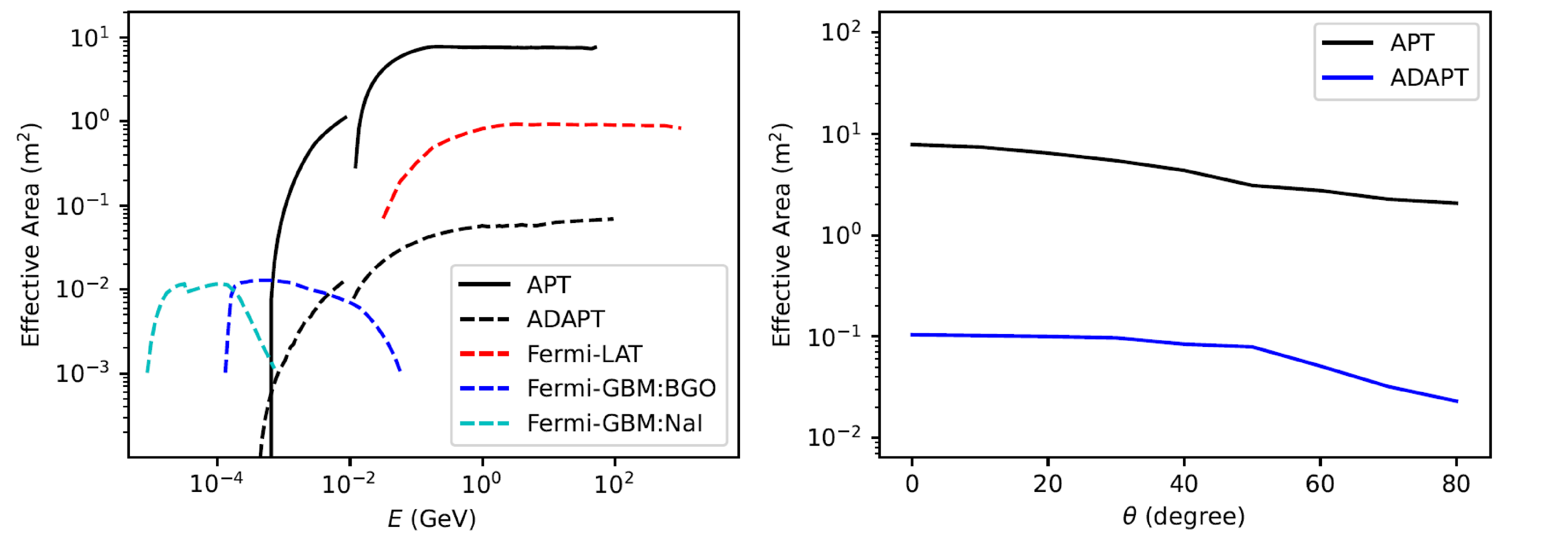

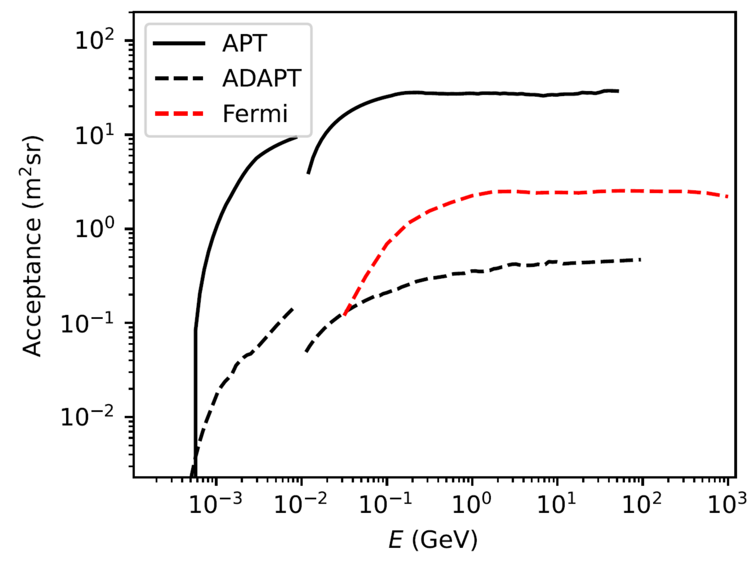

Top: Effective area of APT and ADAPT. Left: The plot shows the normal-incident effective area as a function of gamma ray energy E. Right: The effective area is plotted as a function of inclination angle θ for 1 GeV gamma rays.

Bottom: Geometric factor (acceptance) of APT and ADAPT: The geometric factor is defined as the effective area integrated over the solid angle. The plot shows the geometric factor as a function of gamma ray energy E.

• Point Spread Functions (PSFs)

- The PSFs for APT and ADAPT are determined by the angular offset $\Delta\theta$ between the reconstructed and true gamma-ray directions. The PSFs depend on the energy of the incoming photon (E) and the inclination angle (θ), but do not vary significantly with the azimuthal angle φ.

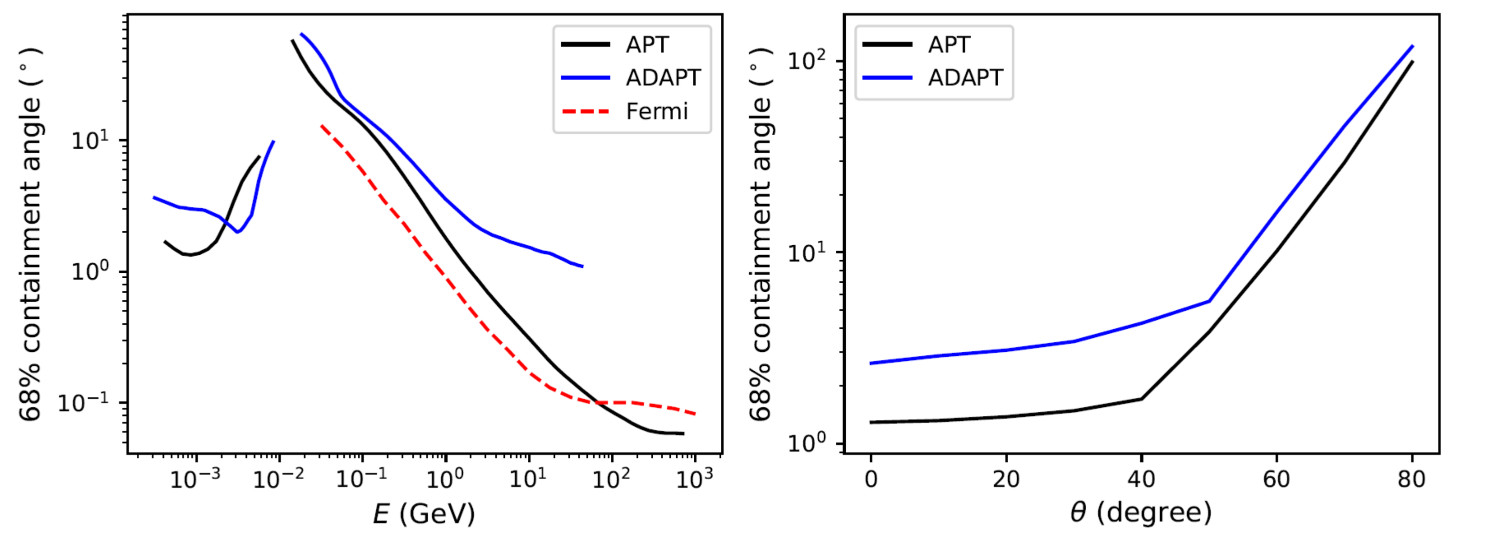

Angular resolution of APT and ADAPT. Left: The plot shows the acceptance-weighted 68% containment angle of $\Delta\theta$ as a function of gamma ray energy E. Right: $\Delta\theta$ is plotted as a function of inclination angle θ for 1 GeV gamma rays.

- Similarly to Fermi-LAT PSFs, the distribution of angular offset between the reconstructed and true gamma-ray directions can be described by the Moffat function. For each specific E and θ, the function parameters are fitted to the reconstruction results to generate the PSFs for APT and ADAPT.

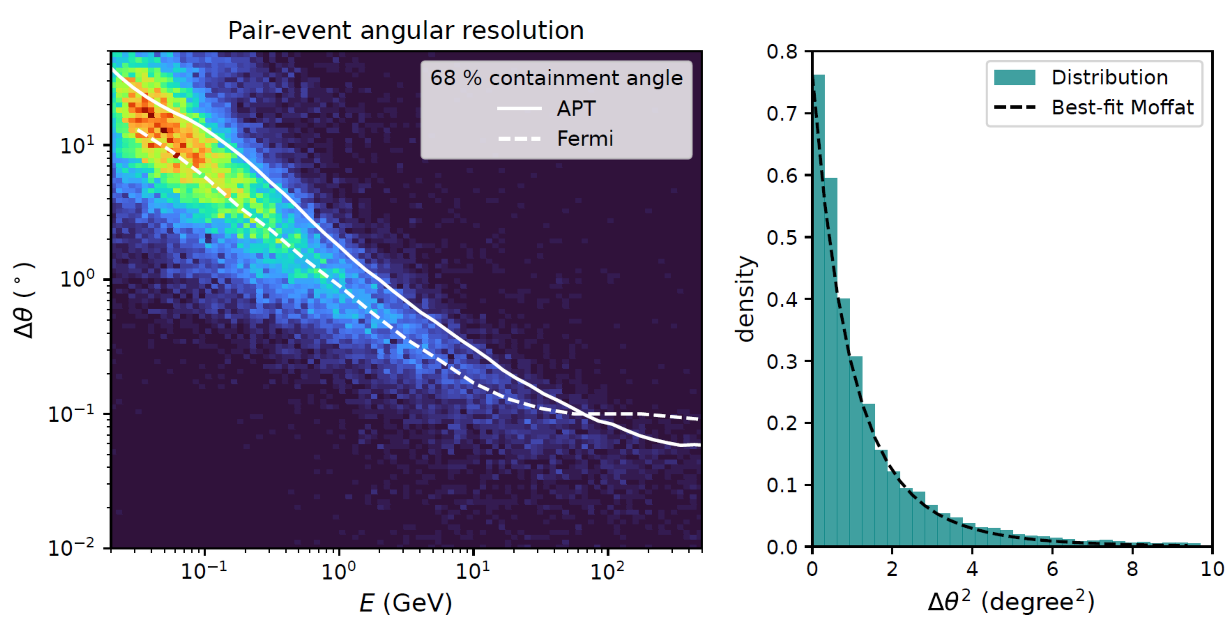

Left: Distribution of $\Delta\theta$ as a function of E for APT.

Right: Distribution of count rate in each uniform $\Delta\theta$ bin as a function of $\Delta\theta$ for APT at 1 GeV. The dashed curve shows the best-fit Moffat function to this distribution.

• Energy Dispersion

- The energy dispersion is measured as the fractional difference between the reconstructed (E') and the true energy (E). We evaluated $\Delta E/E$ (where $\Delta E = |E - E'|$) based on E and θ. To achieve a large area but limited by the payload capacity of the launch vehicles, the APT calorimeter, with 5.4 CsI radiation lengths (approximately 5.8 including fibers and supports), is significantly shallower than the Fermi-LAT ∼10 radiation lengths.

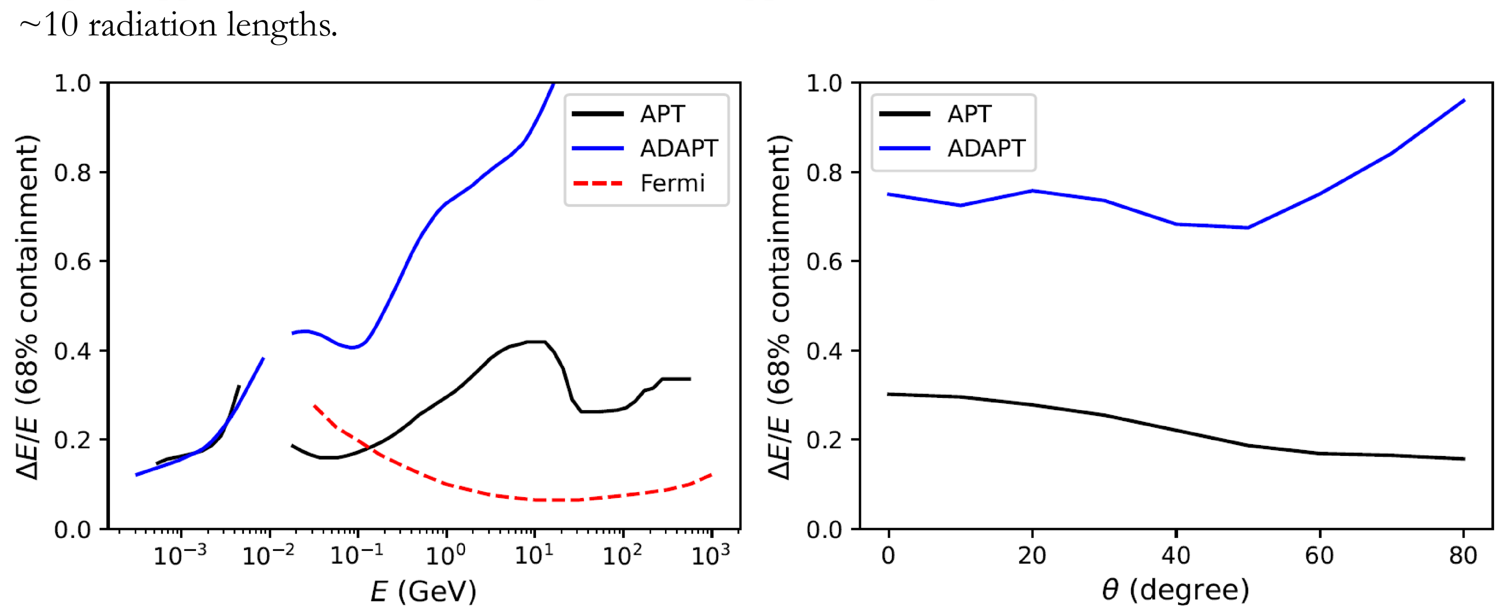

Energy resolution of APT and ADAPT. Left: The plot shows the acceptance-weighted 68% containment of $\Delta E/E$ as a function of gamma ray energy E. Right: $\Delta E/E$ is plotted as a function of inclination angle θ for 1 GeV gamma rays.

† Corrado Altomare[12], Matthew Andrew[5], Blake Bal[7], Richard G. Bose[7], Dana Braun[7], James H. Buckley[7], Jeremy Buhler[2], Eric Burns[4], Roger D. Chamberlain[2], Wenlei Chen[6], Michael L. Cherry[4], Leonardo Di Venere[12], Jeffrey Dumonthier[13], Manel Errando[7], Stefan Funk[10], Priya Ghosh[8], Francesco Giordano[9], Jonah Hoffman[7], Ye Htet[2], Zachary Hughes[7], Aera Jung[5], Patrick L. Kelly[6], John F. Krizmanic[13], Makiko Kuwahara[3], Francesco Licciulli[12], Gang Liu[16], Leonarda Lorusso[9], Mario Nicola Mazziotta[12], John Grant Mitchell[11], John W. Mitchell[1], Georgia A. de Nolfo[11], Giuliana Panzarini[15], Richard Peschke[5], Riccardo Paoletti[17], Roberta Pillera[15], Brian Rauch[7], Davide Serini[12], Garry Simburger[7], Marion Sudvarg[2], George Suarez[13], Teresa Tatoli[11], Gary S. Varner[5], Eric A. Wulf[14], Adrian Zink[10], and Wolfgang V. Zober[7]

1. Astroparticle Physics Laboratory, NASA/GSFC, Greenbelt, MD 20771, USA. 2. Department of Computer Science & Engineering, Washington University, St. Louis, MO 63130-4899, USA. 3. Department of Engineering, University of Hawai'i at M¯anoa, Honolulu, HI 96822, USA. 4. Department of Physics and Astronomy, Louisiana State University, Baton Rouge, Louisiana 70803, USA. 5. Department of Physics and Astronomy, University of Hawai'i at M¯anoa, Honolulu, HI 96822, USA. 6. Department of Physics, Oklahoma State University, Stillwater, OK 74078, USA. 7. Department of Physics and McDonnell Center for the Space Sciences, Washington University, St. Louis, MO 63130, USA. 8. Department of Physics, Catholic University of America, Washington DC, 20064. 9. Dipartimento di Fisica "M. Merlin" dell'Università e del Politecnico di Bari, I-70126 Bari, Italy. 10. Friedrich-Alexander-Universität Erlangen-Nürnberg, Erlangen Centre for Astroparticle Physics, D-91058 Erlangen, Germany. 11. Heliospheric Physics Laboratory, NASA/GSFC, Greenbelt, MD 20771, USA. 12. Istituto Nazionale di Fisica Nucleare, Sezione di Bari, I-70126 Bari, Italy. 13. NASA Goddard Space Flight Center, Greenbelt, MD 20771, USA. 14. Naval Research Laboratory, Washington, DC 20375, USA. 15. Politecnico di Bari, Department of Mechanics, Mathematics and Management, via Orabona, 4, I-70125 Bari, Italy. 16. SLAC National Accelerator Laboratory, 2575 Sand Hill Rd, Mailstop 0094, Menlo Park, CA 94025, USA. 17. Università di Siena and INFN Pisa, I-53100 Siena, Italy.